Friction stir butt welding of strain-hardened aluminum alloy with high strength steel

Article *in* Materials Science and Engineering A · September 2018

DOI: 10.1016/j.msea.2018.09.035

CITATIONS
0

READS
152

4 authors:

Tianhao Wang
University of North Texas
13 PUBLICATIONS **34** CITATIONS
SEE PROFILE

Mageshwari Komarasamy
University of North Texas
38 PUBLICATIONS **161** CITATIONS
SEE PROFILE

K. Liu
University of North Texas
15 PUBLICATIONS **14** CITATIONS
SEE PROFILE

Rajiv S. Mishra
University of North Texas
403 PUBLICATIONS **13,134** CITATIONS
SEE PROFILE

Materials Science & Engineering A 737 (2018) 85–89

Contents lists available at ScienceDirect

Materials Science & Engineering A

journal homepage: www.elsevier.com/locate/msea

Short communication

Friction stir butt welding of strain-hardened aluminum alloy with high strength steel

Tianhao Wang, Mageshwari Komarasamy, Kaimiao Liu, Rajiv S. Mishra*

Center for Friction Stir Processing and Advanced Materials Manufacturing Processes Institute, Department of Materials Science and Engineering, University of North Texas, Denton, TX 76203, USA

ARTICLE INFO

Keywords:
Friction stir welding
Dissimilar
High strength steel
Stress concentration
Digital image correlation

ABSTRACT

Dissimilar metal joining is challenging because of intermetallic compound (IMC) formation. Solid state welding techniques provide an opportunity. 5083-H116 aluminum alloy and HSLA-65 steel sheets were butt welded by friction stir welding. Joint strength and failure position were determined by IMC thickness and stress concentration at welded interface.

1. Introduction

Combination of Al and steel has attracted significant attention because of its great application potential in industry due to light weighting requirements [1–3]. Solid state joining methods such as friction stir welding (FSW) [4], friction welding [5] and hybrid metal extrusion and bonding [6] with lower welding heat input have been favored as compared with conventional fusion welding techniques. Limited chemical reaction and diffusion between Al and steel generally leads to reduced intermetallic compound (IMC) formation during solid state joining. Among these solid state welding techniques, FSW has become an enabling method for joining dissimilar materials [7]. However, weld defects during FSW appear due to the significant differences between thermal expansion coefficients and other thermo-physical properties of Al and steel.

5XXX aluminum alloys have been applied widely in automobile and marine industries because of their high specific strength, formability, and high corrosion resistance [8]. High strength low alloy (HSLA) steel is one of the most used structural steels [8]. Previously, FSW has been used to join 5083 [2,9] and 5186 [8] aluminum alloy with mild steel, and 5052 aluminum alloy with HSLA steel [10]. IMC thickness ranged from 0.25 to 5 μm during friction stir butt welding of aluminum alloy to steel [4,9,11,12], and joint strength decreased with increase in IMC thickness [12]. Generally, the failure position was located at the Al/steel interface, although IMC thickness was significantly reduced as compared with fusion welding. In addition, fatigue properties of Al/steel joint were ~30% lower than that of the base Al and failure position was located at the Al/steel interface [3]. To solve problems above, critical welding parameters (rotation rate and traverse speed) and welding conditions (tool offset and sheet thickness difference) were evaluated in this study. A 5083-H116 aluminum alloy was friction stir welded with HSLA-65 steel to establish a relationship between IMC thickness and joint strength. Stress concentration at the steel/weld nugget during tensile testing was observed.

2. Experiments

AA5083-H116 (strain hardened AA5083) sheet (thickness = 6.0 mm) and HSLA-65 steel sheet (thickness = 5.75 mm) were friction stir butt welded using a W-Re tool. Steel was placed on the advancing side (AS) (Fig. 1(a)). The tool was shifted from Al/steel interface to Al side by 2.5 mm, and thickness of the Al sheet was higher than that of steel sheets by 0.25 mm (Fig. 1(b)). A W-Re tool with threaded conical pin was used (Fig. 1(c)). Pin length, pin diameter at root and tip, and shoulder diameter were 3.8 mm, 7.6 mm, 5.0 mm, and 16.0 mm, respectively (Fig. 1(d)). Standard tensile testing (ASTM E8-04) and mini-tensile testing were conducted to evaluate Al/steel joint strength and weld nugget strength, respectively (Fig. 1(e)). The width, thickness and gage length of the mini tensile samples were 1.0, 0.6, and 2.0 mm, respectively. Scanning electron microscopy was applied for observing horizontal and cross section of welded Al and steel sheets. Electron backscatter diffraction (EBSD) and Image J were used to measure the matrix grain size and volume fraction of steel fragments, respectively. 3D features were analyzed using the Robo-Met. 3D (R) system for automated serial sectioning and the MIPAR software for post processing and images. Welding parameters and conditions including

* Corresponding author.
E-mail address: Rajiv.Mishra@unt.edu (R.S. Mishra).

https://doi.org/10.1016/j.msea.2018.09.035
Received 21 May 2018; Received in revised form 10 September 2018; Accepted 11 September 2018
Available online 12 September 2018
0921-5093/

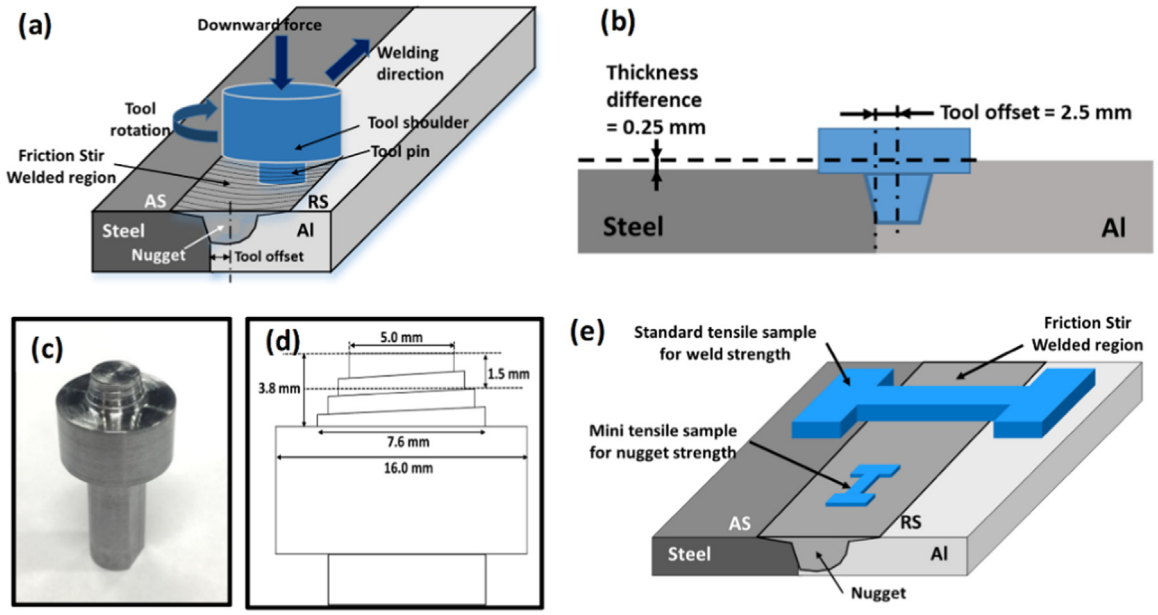

Fig. 1. (a) Schematic of FSW of aluminum and steel sheets, (b) schematic of the cross-section displaying tool offset and sheet thickness difference, (c) photograph of a W-Re tool, (d) dimensions of the W-Re tool, and (e) schematic of fabrication of standard E8 tensile and mini-tensile samples.

Table 1
Summary of welding parameters for joints 1–6.

Joint number	R (rpm)	T (mm/min)	P_d (mm)	TO (mm)	TD (mm)
1	500	5	4.2	2.5	0.25
2	500	10	4.2	2.5	0.25
3	500	15	4.2	2.5	0.25
4	500	20	4.2	2.5	0.25
5	700	10	4.2	2.5	0.25
6	700	20	4.2	2.5	0.25

rotation rate (R), traverse speed (T), plunge depth (P_d), tool offset (TO) and thickness difference (TD) of six runs are listed in Table 1. Two-dimensional (2D) digital image correlation (DIC) was applied for localized deformation measurements during standard tensile testing on dissimilar Al/steel joints.

3. Results and discussion

During FSW with tool offset in Al, only tool shoulder and small volume of pin cut the steel. Note that while the aluminum is plasticized at the welding temperature and can flow, the steel is relatively rigid. The horizontal plane of the welded sample at the exit hole is shown in Fig. 2(a). Steel is cut into pieces and moved by the rotating tool from the front side of the pin to the back side of the pin. The Al nugget along with steel fragments form a composite nugget, in which processed aluminum was the matrix and steel fragments were reinforcement particulates. After FSW and subsequent recrystallization, 5083-H116 lost its work-hardened strength due to thermal softening. In addition, aluminum during the welding process underwent expansion and contraction. Therefore, thicker aluminum sheets were applied to provide excessive aluminum to countervail contraction after welding. Among the welding parameters listed in Table 1, R and T were critical to control defect formation. The basic mechanism of defect formation during FSW of Al and steel is shown in Fig. 2(b). Combination of low R and high T led to poor material flow around the rotating pin and contributed to lack of fill void formation (Fig. 2(c_1) and (c_3)). On the other hand, high R and low T that led to excessive aluminum expansion during welding and aluminum contraction after welding contributed to hot crack formation (Fig. 2(c_2) and (c_3)). 3-dimensional (3D) images show the Al/steel joint (Fig. 2(d_1)), steel fragments of various sizes in the weld nugget (Fig. 2(d_2)) and a through lack of fill void at the bottom of the weld nugget next to the nugget/steel boundary (Fig. 2(d_3)). Volume fraction of steel fragments in nugget of joint 3 is ~12% (Fig. 2(e_2)). Note that black particles in Fig. 2(e_2) indicate the steel fragments. Grains in aluminum matrix in nugget of joint 3 are shown in Fig. 2(e_3), grain size distribution in shown in Fig. 2(e_4), and the average grain size is ~2.5 μm.

With R of 500 rpm and T of 5, 10 and 15 mm/min, joints 1, 2 and 3 were produced without defects. Standard tensile tests were conducted on joints 1–3 and base aluminum alloy and steel. All the joints (1–3) fractured at the weld nugget/steel boundary where IMC existed. Joint strength increased with reduction in IMC layer thickness (Fig. 3(a) and (b)). Note that stress concentration also existed at the nugget/steel boundary due to substantial difference in modulus and strength of weld nugget and steel, which leads to crack initiation and propagation (Fig. 3(e)). It shows that the property mismatch between base materials reduced due to the weld nugget (Fig. 3(c) and (d)). Compared with friction stirred AA5083-H116, the Al/steel weld nugget was enhanced due to the existence of dispersed steel fragments. Hall-Petch effect and load transfer effect can be applied to calculate the strength increase:

$$\Delta\sigma_{H-P} = k_y d^{-1/2} \quad (1)$$

$$\Delta\sigma_{LT} = \frac{1}{2} v_p \sigma_m \quad (2)$$

where $\Delta\sigma_{H\text{-}P}$ is stress increase based on the Hall-Petch effect, k_y is the strengthening coefficient, d is average grain size, $\Delta\sigma_{LT}$ is stress increase based on loading transfer effect, v_p is the volume fraction of particles and σ_m is yield strength of the unreinforced matrix. k_H (constant associated with hardness measurements) for AA5083 is ~33 HV $\mu m^{1/2}$ [13], which can be converted to $k_y \approx 99$ MPa $\mu m^{1/2}$ ($k_y \approx 3k_H$, [14]). For joint 3, nugget grain size, d was ~2.5 μm, v_p was ~12%, and σ_m was ~200 MPa. Therefore, $\Delta\sigma_{H\text{-}P} \approx 70$ MPa and $\Delta\sigma_{LT} \approx 12$ MPa were obtained based on Eqs. (1) and (2). The combined strength increase was ~82 MPa, which fits with the strength increase from friction stirred AA5083-H116 to weld nugget (Fig. 3(c) and (d)). Note that the process parameters for friction stirred AA5083-H116 are same with the parameters for joint 3 and that σ_m was obtained from friction stirred AA5083-H116 specimen. In addition, AA5083-H116 has higher

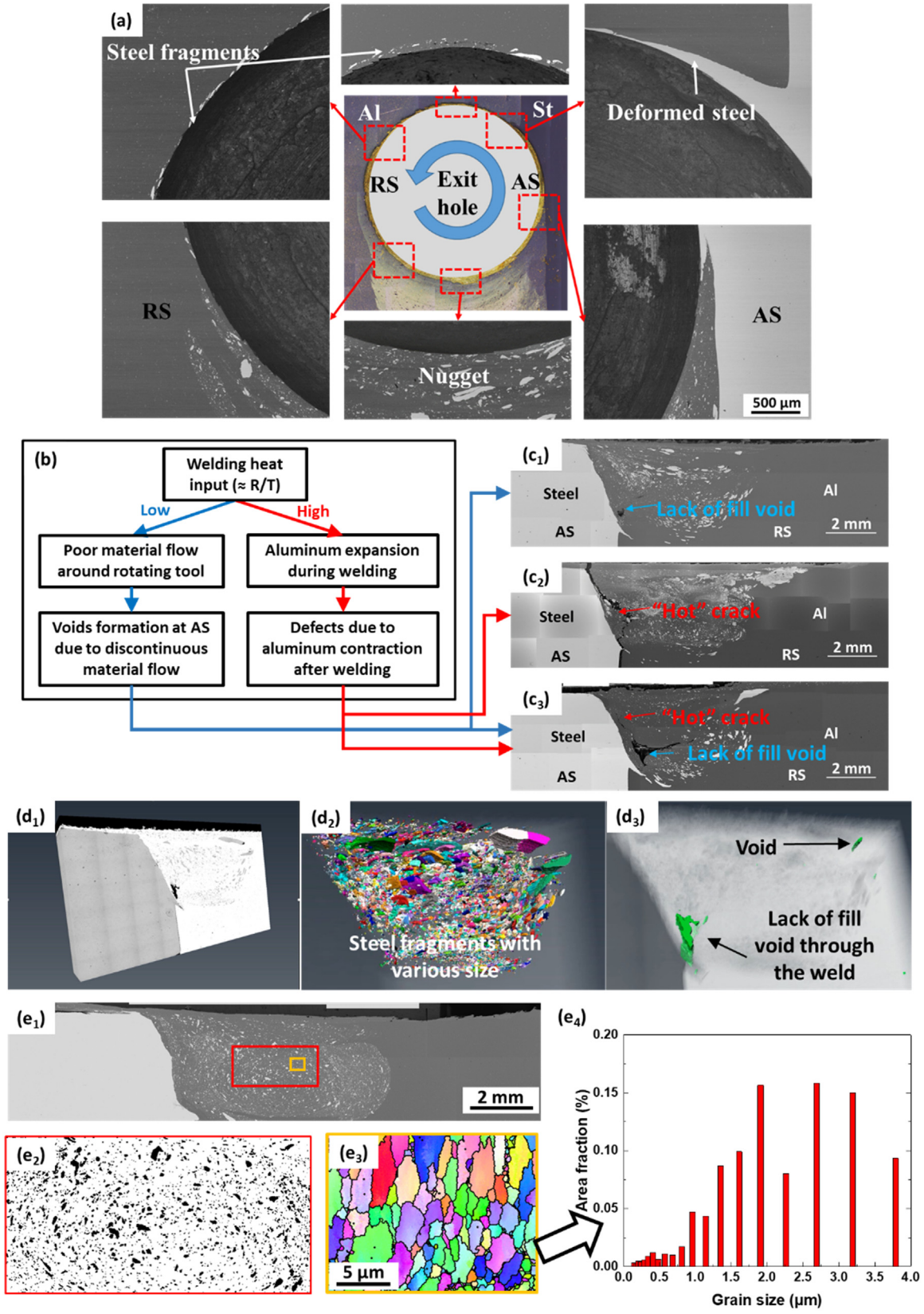

Fig. 2. (a) Horizontal plane at key hole showing material flow during FSW, (b) basic mechanisms of effect of rotation rate and traverse speed on defect formation during Al/steel butt welding, cross-section images of dissimilar joints of (c_1) joint 4 (R500T20), (c_2) joint 5 (R700T10) and (c_3) joint 6 (R700T20), (d_1) 3-D image showing Al/steel butt joint with (d_2) steel fragments in the weld nugget with various sizes and (d_3) a through lack of fill void, (e_1) cross-section image of joint 3 (e_2) measurement image of selected region with red rectangle in Fig. 2(e_1) via Image J, (e_3) EBSD IPF image of selected region with yellow rectangle in Fig. 2(e_1) and (e_4) distribution of grain size in Fig. 2(e_3). (For interpretation of the references to color in this figure legend, the reader is referred to the web version of this article).

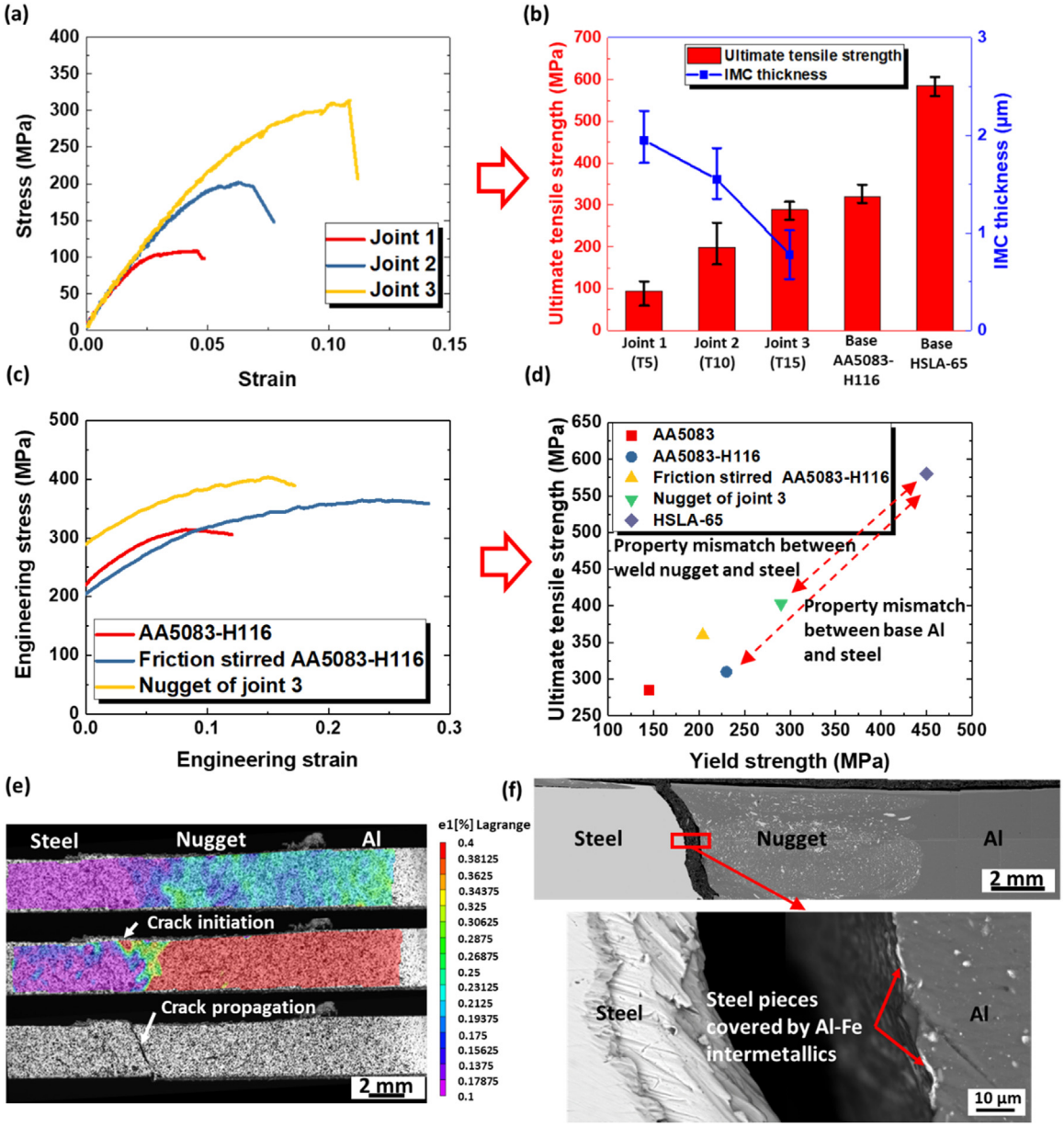

Fig. 3. (a) Stress-strain curves of dissimilar joints 1–3, (b) ultimate tensile strength of dissimilar joints 1–3, base AA5083-H116 and HSLA-65 and thickness of intermetallic compound of joints 1–3, (c) engineering stress-strain curves of base and friction stirred AA5083-H116 and weld nugget of joint 3, (d) comparison of ultimate tensile strength and yield strength of base AA5083-H116, base HSLA-65, weld nugget of joint 3 and friction stirred AA5083-H116, (e) 2D DIC analysis on the cross section of joint 3 during testing, and (f) cross section of fractured joint 3.

strength than AA5083 due to work-hardening. Al/steel joints fractured along the boundary between weld nugget and steel (Fig. 3(f)). In the enlarged picture, steel pieces covered by Al-Fe IMC are observed along the fracture path in the Al part, which is detrimental to joint strength.

4. Conclusions

(1) Tensile testing of Al/steel joints showed that stress concentration and brittle IMC at the boundary between weld nugget and steel led to crack initiation and propagation. The strength of defect-free joints increased with reduction in IMC thickness. Among the FSW parameters evaluated in this study, the tool rotation rate of 500 rpm and traverse speed of 15 mm/min gave the best joint strength of ~289 MPa (90% of base aluminum alloy).

(2) Strength of weld nugget was enhanced by the existence of dispersed steel fragments as compared with base Al alloy. The measured strength increase in the nugget matches with calculations based on grain boundary strengthening and composite strengthening.

Acknowledgments

This work was supported under the US National Science Foundation-Industry University Copperative Research Centers Program (NSF-IUCRC) grant for Friction Stir Processing (NSF-IIP 1157754). We also acknowledge the University of North Texas Materials Research Faculty (MRF) and UES Inc. (Dayton OH USA).

Data availability statement

The raw/processed data required to reproduce these findings cannot be shared at this time as the data also forms part of an ongoing study.

References

[1] S. Ramasamy, Drawn arc stud welding: crossing over from steel to aluminum, Weld. J. 79 (2000) 35–39.

[2] T. Watanabe, H. Takayama, A. Yanagisawa, Joining of aluminum alloy to steel by friction stir welding, J. Mater. Process. Technol. 178 (2006) 342–349.

[3] H. Uzun, C. Dalle Donne, A. Argagnotto, T. Ghidini, C. Gambaro, Friction stir welding of dissimilar Al 6013-T4 to X5CrNi18-10 stainless steel, Mater. Des. 26 (2005) 41–46.

[4] W. Lee, M. Schmuecker, U.A. Mercardo, G. Biallas, S. Jung, Interfacial reaction in steel–aluminum joints made by friction stir welding, Scr. Mater. 55 (2006) 355–358.

[5] S.D. Meshram, T. Mohandas, G.M. Reddy, Friction welding of dissimilar pure metals, J. Mater. Process. Technol. 184 (2007) 330–337.

[6] L. Sandnes, Ø. Grong, J. Torgersen, T. Welo, F. Berto, Exploring the hybrid metal extrusion and bonding process for butt welding of Al–Mg–Si alloys, Int. J. Adv. Manuf. Technol. (2018) 1–7.

[7] N. Kumar, W. Yuan, R.S. Mishra, Friction Stir Welding of Dissimilar Alloys and Materials, (2015) (ISBN: 978-0-12-802418-8).

[8] M. Dehghani, A. Amadeh, S.A. Mousavi, Investigations on the effects of friction stir welding parameters on intermetallic and defect formation in joining aluminum alloy to mild steel, Mater. Des. 49 (2013) 433–441.

[9] K. Kimapong, T. Watanabe, Friction stir welding of aluminum alloy to steel, Weld. J. 83 (2004) 277–282.

[10] K. Ramachandran, N. Murugan, S.S. Kumar, Effect of tool axis offset and geometry of tool pin profile on the characteristics of friction stir welded dissimilar joints of aluminum alloy AA5052 and HSLA steel, Mater. Sci. Eng. A 639 (2015) 219–233.

[11] W. Jiang, R. Kovacevic, Feasibility study of friction stir welding of 6061-T6 aluminium alloy with AISI 1018 steel, Proc. Inst. Mech. Eng. Part B J. Eng. Manuf. 218 (2004) 1323–1331.

[12] T. Tanaka, T. Morishige, T. Hirata, Comprehensive analysis of joint strength for dissimilar friction stir welds of mild steel to aluminum alloys, Scr. Mater. 61 (2009) 756–759.

[13] T. Hirata, T. Oguri, H. Hagino, T. Tanaka, S.W. Chung, Y. Takigawa, K. Higashi, Influence of friction stir welding parameters on grain size and formability in 5083 aluminum alloy, Mater. Sci. Eng. A 456 (2007) 344–349.

[14] Y.S. Sato, M. Urata, H. Kokawa, K. Ikeda, Hall–Petch relationship in friction stir welds of equal channel angular-pressed aluminium alloys, Mater. Sci. Eng. A 354 (2003) 298–305.